All Polarization Maintaining Brillouin Erbium-Doped Fiber Laser With Sub-kHz Linewidth Using Saturated Absorber and Self-Injection Feedback

Junsen Yang, Zhengkang Wang, Jianming Shang, Shiyou Xiao, Zhixue Li, Bin Luo, Tianwei Jiang, and Song Yu

***Abstract*—A narrow-linewidth all-polarization-maintaining (PM) Brillouin erbium-doped fiber laser (BEFL) is proposed and demonstrated experimentally, which employs erbium-doped fiber (EDF) acting as both the linear gain and the Brillouin gain medium. In order to realize a single longitudinal mode (SLM) operation and a narrow linewidth fiber laser output, the saturable absorber (SA) and the optical self-injection feedback structure are employed in the BEFL for the first time. In this experiment, three sets of comparative experiments are conducted to demonstrate the effectiveness of the SA and the self-injection feedback structure. The experimental result shows that the SA structure can eliminate transient multimode phenomena and narrow the linewidth, and the self-injection feedback structure can act as an effective mode filter and a compound-cavity to make the intracavity mode purer. A stable SLM operation of the BEFL is verified by the delayed self-heterodyne system, which thanks to the adding of the SA and the self-injection feedback structure. The BEFL's wavelength stability detected by is less than 0.0045 nm over 14 hours. In addition, an ultra-narrow linewidth of approximately 224 Hz is obtained.**

***Index Terms*—Brillouin erbium-doped fiber laser (BEFL), saturable absorber (SA), self-injection feedback structure.**

I. Introduction

SLM erbium-doped fiber lasers (EDFLs) have the characteristics of narrow bandwidth, low noise and high stability. Consequently, SLM EDFLs are widely used in high precision fiber sensing, remote coherent optical communication, high-resolution radar imaging and other fields [1], [2], [3], [4]. Up to now, SLM EDFLs mainly have two kinds of cavity structures: the linear cavity [5] and the ring cavity [6], [7]. Due to the short length of the linear cavity, the linear cavity fiber laser is not easy to generate mode hopping state [8], [9], [10], though it can achieve long-term stable SLM operation. By comparison, the ring cavity fiber laser has longer cavity length, which can produce laser with lower noise and narrower linewidth [11], [12], [13], [14]. However, the longer cavity length leads to the reduction of mode spacing, which makes it easy to achieve the mode hopping operation [15].

In recent years, the Brillouin fiber laser based on the stimulated Brillouin scattering (SBS) has attracted significant interest [16]. At present, there are mainly three types of Brillouin gain medium fibers: the single-mode fiber [17], [18], the high nonlinear fiber [19] and the EDF [20], [21]. Serving as the gain medium, the single-mode fiber has the characteristics of low price and stable excitation SBS. However, the length of the single-mode fiber usually requires several kilometers, which lead to mode hopping operation due to the short mode spacing in the cavity [17], [18]. As a comparison, only a few meters of the high nonlinear fiber is requied to excite SBS, which can increase the mode spacing and reduce the phenomenon of the mode hopping. However, the power of the laser is too low due to the large loss coefficient of the high nonlinear fiber [19]. Compared to the two types of optical fibers mentioned above, the EDF has been proposed as Brillouin gain medium in recent years, which can excite the SBS with a few mW power of the Brillouin pumped (BP). BEFL has the characteristics of low threshold and easy excitation [20]. The output station of the BEFL strongly depends on the power of the BP. When the power of the BP exceeds the threshold of the SBS, stokes light resonates and amplifies in the cavity [20]. Compared with other scattering effects, SBS has the characteristics of low threshold, high gain and narrow spectral width. Therefore, SBS can be applied in narrow-linewidth lasers. However, free running BEFL exhibit transient multimode phenomena, requiring additional filtering methods to achieve stable SLM operation.

In this article, we propose an all-PM BEFL based on the SA and the self-injection feedback structure, which is the first time proposed on our knowledge. The all-PM structure can suppress the interference of the environment and improve the practicability of the system [21]. In the cavity, the SA serves as a dynamic Bragg grating to suppresses the transient multimode phenomenon and to achieve a stable SLM state. Moreover, the self-injection feedback structure is employed as an mode filter and and a compound-cavity to make the intracavity mode purer. As for the output performance of the BEFL, we achieved an all-PM SLM BEFL with a ultra-narrow linewidth of 224 Hz and an excellent wavelength stability of $<$4.5 pm.

Manuscript received 16 November 2023; revised 24 January 2024; accepted 31 January 2024. Date of publication 6 February 2024; date of current version 1 March 2024. This work was supported in part by the National Natural Science Foundation under Grant 61531003, Grant 61690195, Grant 61701040, and Grant 61427813, and in part by the Fundamental Research Funds of BUPT under Grant 2022RC08–500422353 and Grant 2022RC10-500422355. *(Corresponding author: Jianming Shang.)*

The authors are with the Beijing University of Posts and Telecommunications, Beijing 100088, China (e-mail: shangjamin@bupt.edu.cn).

Digital Object Identifier 10.1109/JPHOT.2024.3362819

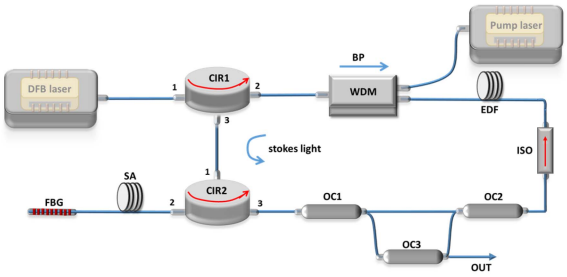

Fig. 1. Configuration of the proposed BEFL. CIR: circulator. WDM: wavelength division multiplexing. EDF: erbium-doped fiber. SA: saturable absorber. FBG: fiber bragg grating. OC: optical coupler.

II. Experimental Setup and Principle

A. Configuration of BEFL

The experimental setup of the all-PM SLM BEFL is illustrated in Fig. 1. The all-PM structure is adopted to guarantee the practicability of the system. The BP employed is a standard distributed feedback (DFB) laser with a maximum power of 15.5 dBm and a linewidth of approximately 3 kHz. After passing through an optical circulator (CIR1), the BP excites SBS in 4-m-long PM commercialized EDF. The EDF (EDF1, IXF-EDF-FGL-PM-L3) serves as the linear gain medium is pumped by the LD with the maximal power of 400 mW. When the power of the BP exceeds the threshold of SBS in the EDF, the power of the stokes light will increase significantly. After traversing the EDF, the BP is blocked by the isolator and the backward-propagating stokes light can be cycled amplification in the cavity. Since the Brillouin gain coefficient of EDF is too small, the total gain at stokes wavelength is less than the maximum linear gain of EDF. In addition, the wavelength of the laser is around 1530 nm due to the maximum gain wavelength of EDF is 1530 nm [20]. The coarse filter structure can be constructed by using the CIR2 and the fiber Bragg grating (FBG). The center wavelength, reflectivity and 3-dB bandwidth of the PM FBG is 1549.41 nm, 99.33% and 0.22 nm, respectively. The SA is utilized as an coarse filter structure to suppress the amplified stimulated emission (ASE) noise beyond the bandwidth. Because the gain of EDF can be approximately considered uniform in the bandwidth, the total gain superimposed at the stokes light wavelength is the largest.

To achieve SLM operation and improve the mode rejection ratio, we implemented a 2-m-long EDF (EDF, IXF-EDF-FGL-1480-PM) as the SA. When the power of the BP exceeds the threshold of the SBS, counterclockwise propagating stokes light is generated. The mode of the stokes light automatically matches with the resonant mode in the cavity. The self-injection feedback structure composed of optical coupler (OC2 and OC3), which has filtering function that make the intracavity mode purer. The laser output is extracted from the 90% port of the PM OC3 with a coupling ratio of 90:10.

The working principle of the BEFL is depicted in Fig. 2(a). The gain spectrum of EDFA is uneven and the maximum gain wavelength is the point a. When the power of the BP exceeds the threshold of the SBS, stokes light is generated at wavelength of the point b. Because the total gain at the point b is higher than the total gain at the point a, the output wavelength of the laser is the point b. However, when the central wavelength of the Brillouin gain spectrum significantly deviates from the maximum gain wavelength of the EDF, the gain at the point c is lower than that at the point a. Consequently, the laser initially oscillates at wavelength of the point a. Because of the uniform broadening property of the EDFA, the gain at wavelength of the point c is decreasing, making the laser unable to operate at wavelength of the point c. At this time, the laser is free running EDFLs [20]. The reflection spectrum of the FBG used in the experiment shown in Fig. 2(b) displays a center wavelength of 1549.41 nm and a 3-dB bandwidth of 0.22 nm. The FBG functions as a reflection filter to complete the original wavelength selection and to reduce the potential longitudinal mode in the cavity. Thanks to the flat gain profile within the FBG, the gain is maximized at the wavelength of the stokes light [20]. The gain spectral width of the SBS is about 20 MHz, it is usually necessary to ensure that the cavity length is less than 10 m.

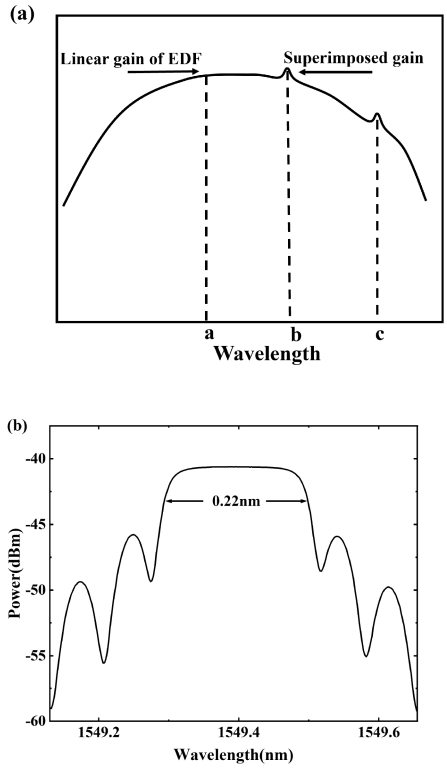

Fig. 2. (a) Principle of BEFL. (b) Reflection spectrum of FBG.

B. Operation Principle of Reflective Saturated Absorber

The filtering bandwidth is an important performance indicator of saturated absorber structures, which is usually calculated using the transfer matrix method. The transfer function of the SA composed of Sagnac ring is solved by the transfer matrix [21], [22]. As shown in Fig. 3, the derivation of the reflective saturable absorber (RSA) is partially different. Because the length of single-mode fiber is too short, the loss coefficient is ignored in the calculation. Where β L=n ω L/c=2$\pi\nu$nL/c is the increment of phase, L_1 and L_2 is the length of single-mode fiber, E_{1-1}^{in}

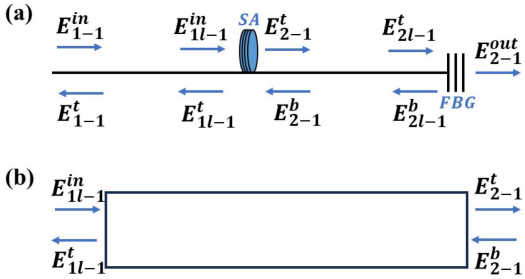

Fig. 3. (a) Light propagation structure diagram of SA. (b) Light propagation diagram of equivalent uniform bragg grating.

is the first input light intensity, E^{in}_{1l-1} is the input SA light intensity, E^{t}_{2-1} is the output SA light intensity, E^{t}_{2l-1} is input FBG light intensity, Other light intensity symbols have similar meanings. Unlike Sagnac ring structure, the light intensity at both ends of the SA is not the same every time independently. The transmission function of the dynamic fiber grating (DFG) formed in SA changes. The DFG is first formed by a round trip of initial light intensity and incident light. Under the action of this grating, E^{t}_{2-1} and E^{b}_{2-1} will change, which will lead to the change of DFG and eventually become stable with the increase of the number of iterations. As the model of DFG, the transmission matrix expression of the uniform grating $H_{grating}$ (1) as follows:

$$H_{\text{grating}} = \frac{1}{F_{22}} \begin{Bmatrix} F_{12} & 1 \\ 1 & F_{12} \end{Bmatrix} \tag{1}$$

As the number of iterations of reflected light increases, the dynamic grating properties formed gradually stabilize. The transfer function is shown in (2).

$$\frac{E^{t}_{1^{\sim}l}}{E^{in}_{1^{\sim}l}} <= \left| \frac{1}{F_{22}^2} e^{j\beta(2L_2)} \right| + \left| \frac{F_{12}}{F_{22}} \left(1 + \frac{1}{F_{22}^2} e^{j\beta(4L_2)} + \frac{1}{F_{22}^2} F_{12} e^{j\beta(6L_2)} \right) + \cdots \right) \right| \tag{2}$$

Since each iteration only increases the order of the coefficient of $\frac{F_{12}}{F_{22}}$, and F_{12} is always less than F_{22}. With the increase of the order, the coefficients becomes smaller and approaches zero. Furthermore, the approximate expression of the transfer function is as follows:

$$\left| \frac{E^{t}_{1l-n}}{E^{in}_{1^{\sim}l}} \right| \approx \left| \left(\frac{F_{12}}{F_{22}} \right)^2 \right| = \frac{\sinh(\alpha \mathrm{L})^2}{(\cosh(\alpha \mathrm{L}))^2 - \frac{\delta^2}{k^2}} \tag{3}$$

$$\Delta v = \frac{c}{\lambda} \frac{2\Delta n}{n_{eff}\lambda} \sqrt{\left(\frac{\Delta n}{2n_{eff}} \right)^2 + \left(\frac{\lambda}{2n_{eff}L} \right)^2} \tag{4}$$

The transfer functions of the RSA and the Sagnac ring of the SA are approximately the same. The longer the length of the SA, the narrower its filtering bandwidth. However, SA can increase the cavity length and reduce the mode spacing of the laser. To ensure the SLM of the laser, the bandwidth of the SA needs to be smaller than the mode spacing. In this experiment, the length of the SA was adopted as 2 m. Where Δn is the change of refraction index and the value is generally less than 3×10^{-7} [23], [24], λ = 1549.384 nm, L = 2 m, n_{eff} = 1.47 is the effective refraction index of the EDF. The calculated bandwidth $\Delta\nu$ of the SAG is 14.41 MHz. The length of the main cavity is 11 m, and the free spectral range of the intracavity mode is 19.2 MHz. Therefore, the ring laser without BP can achieve SLM.

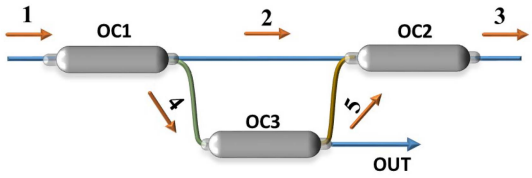

Fig. 4. Structure diagram of the self-injected feedback structure.

C. Self-Injection Feedback Structure

The SA structure ensures that the laser has a stable SLM status and narrow the linewidth [25]. The self-injected feedback structure has filtering function, which can make the mode in the cavity purer [26], [27]. The self-injection feedback structure is illustrated in Fig. 4. The light is divided into two parts by the OC1. One of the components resonates and amplifies within the main cavity, following the 1 to 2 to 3 direction. The other components passes through the OC3, where 90% of the light is output and 10% of the light is injected into the cavity along the 5 direction. On the one hand, long cavity length increases the transmission life of laser. On the other hand, more proportion of light can be guided back into the cavity, thus this structure has a higher Q value and narrower transmission bandwidth [27]. The longer the length of the self-injection feedback structure, the better its feedback effect. However, the self-injection feedback structure also plays a role as compound-cavity, which affects the mode spacing of the laser [28]. Increasing the feedback length will result in a decrease in the mode spacing of the laser, which in turn affects the SLM of the laser. Therefore, the self-injection feedback structure did not adopt a long feedback length in the experiment.

III. Experimental Result and Discussion

A. BEFL Without SA and Self-Injection Feedback Structure

This section discusses the characteristics of the BEFL without the SA and the self-injection feedback structure. As shown in Fig. 1, the SA, OC2 and OC3 components have been omitted and the laser is output from the 50% port of the OC1. When the power of the BP is zero, the laser is a free running EDFLs. Fig. 5(a) shows the results of the laser wavelength using a. The wavelength of the laser is 1549.426 nm, and the OSNR is 72.5 dB without the BP. However, the 0.02 nm resolution of the spectrometer limits ability to accurately determine the state of the laser. Fig. 5(b) shows the SLM state of the laser using the beat frequency method. It is worth noting that the output of the laser is multimode with a mode spacing of 32.5 MHz and the cavity length is 6.7 m. The multimode phenomenon arises from the existence of multiple resonant modes within the bandwidth of the FBG.

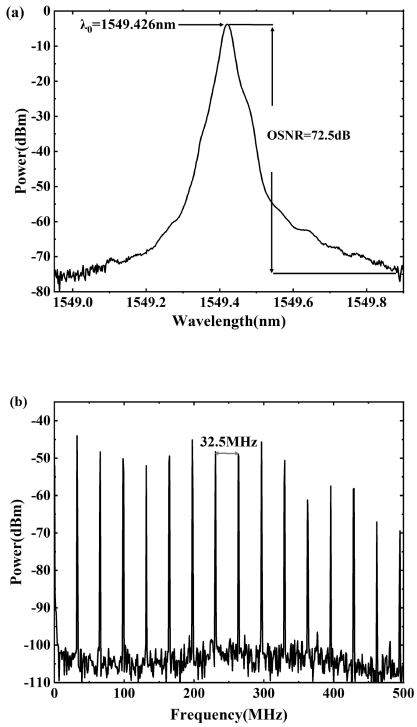

Fig. 5. (a) Spectrogram of free running EDFLs without the SA, self-injection feedback structure and BP. (b) spectrogram diagram of free EDFLs.

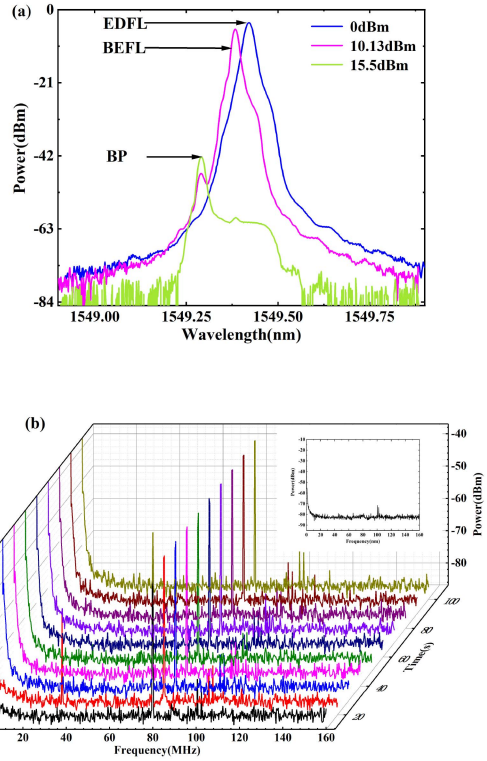

Fig. 6. (a) Spectrogram of the different BP under 120 mw pump. (b) BEFL beat frequency state without the SA and the self-injection feedback structure.

The output state of the BEFL depends on the power of the BP and the 980 nm pump light. When the power of the BP is lower than the threshold of the SBS, the intracavity resonant light and the BP seize the gain of the EDF. Since the power of the BP is too small, the output of the laser is mainly the intracavity resonant light. When the power of the BP exceeds the threshold of SBS, the stokes light is generated in the EDF. The stokes light is rapidly amplified to seize most of the EDF gains and inhibit the generation and amplification of the other modes. As the power of the BP increases, it emerges as the dominant factor in the gain competition, leading to a gradual reduction in the power of the stokes light. The output of the laser is Rayleigh scattering of the BP and the wavelength of the BP is 1549.290 nm in the experiment.

As depicted in Figs. 5(b) and 6(a), the laser is an multimode EDFLs without the BP. When power of the BP increases to 10.13 dBm, stokes light obtain dominant advantage in the gain competition. However, when the power of the BP increases to 15.5 dBm, the output of the BEFL is BP-induced Rayleigh scattering light. This is because excessive BP snatch most of the gain of EDF, making the net gain of stokes light and intracavity resonant light less than zero. The wavelength of the stokes light and Rayleigh scattering light are 1549.384 nm and 1549.290 nm, and the Brillouin frequency shift is 0.094 nm. The cavity length of the BEFL is about 6.7 m, and the corresponding mode spacing is 32.5 MHz. The minimum resolution of the spectrometer is 0.02 nm, corresponding to 2.5 GHz. Therefore, the SLM of the BEFL cannot be observed from the spectrometer. SLM of the BEFL is measured by the delayed self heterodyne method and the results are shown in Fig. 6(b). BEFL can achieve a relatively stable SLM status in short time without additional filter devices. However, transient multimode phenomenon occurs in the measurement. At the 20th second, the power of the other modes suddenly increases forming multimode phenomenon. It is worth noting that the power spike at 100 MHz corresponds to the electrical noise of the photodetector (PD). The upper right corner of Fig. 6(b) displays the photodetector (PD) spectrum without light intensity. With the injection of the BP, the intracavity mode becomes stable gradually and switches to SLM status again. Through 500 statistical analyses of the laser beat frequency, 21 multimode phenomena were observed. However, the BEFL with the SA structure can achieve a stable SLM status for a long time.

The linewidth of the BEFL is measured by the delayed self heterodyne method as shown in Fig. 7(a) [29], [30]. The light of the BEFL is divided into two parts by 50:50 OC. One part is sent through acousto-optic modulator with frequency downshift of 80 MHz and the other part is sent into a 79.8 km delay fiber. The light of two parts beat frequency through the coupler. The optical signal is converted into electrical signal by the PD for observation on the spectrometer. Theoretically, thousands of kilometers of the delay fiber are needed to accurately obtain the linewidth of the BEFL, which is impossible because of the serious $\frac{1}{f}$ noise and excessive attenuation loss. To reduce the measurement error, Lorentz fitting is usually used for the measurement data [14]. As shown in Fig. 7(b), the 20-dB bandwidth of the BEFL is measured to be 17.9 kHz. Thus, the corresponding linewidth of the proposed fiber laser can be estimated to be 900 Hz. SBS can reduce linewidth of the laser to certain extent, but it cannot be

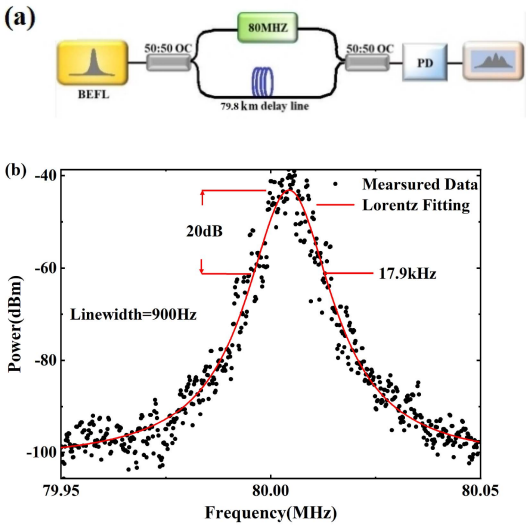

Fig. 7. (a) System architecture of delayed self heterodyne systems. (b) Linewidth measurement diagram of the BEFL without the SA and the self-injection feedback structure.

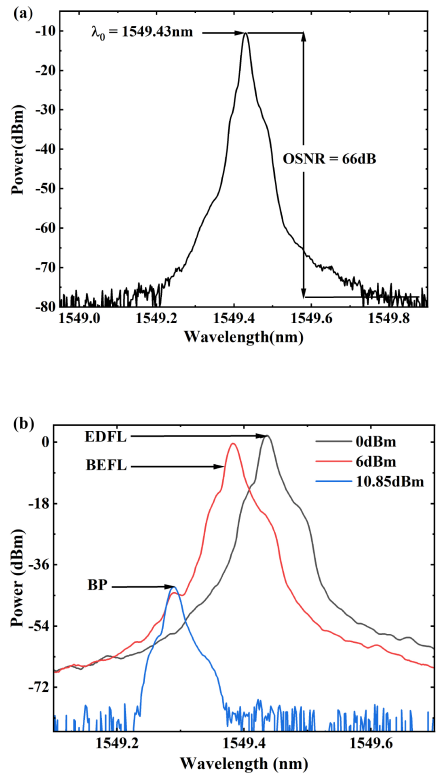

Fig. 8. (a) Spectrogram of EDFLs with the SA without the BP. (b) Spectrogram of the different BP under 120 mw pump.

infinitely reduced. Further reducing the linewidth of the BEFL require some additional measures [19].

B. BEFL With SA Structure

A 2-m SA was employed in the experimental structure. Fig. 8(a) displays the spectrum of the laser without BP. The wavelength of the laser is 1549.432 nm and the OSNR is 66 dB.

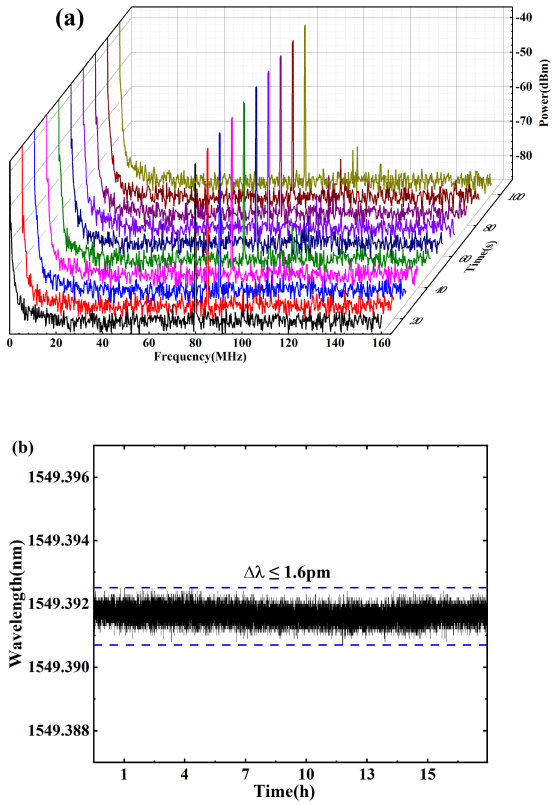

Fig. 9. (a) BEFL beat frequency state with the SA structure. (b) Wavelength test diagram of BEFL with the SA.

As shown in Fig. 8(b), the output state of the laser transitions from EDFLs to BEFL with the BP power increases. When the power of the BP is too high, the stokes light cannot obtain sufficient gain to maintain resonance. Therefore, the output of the laser is Rayleigh scattering light from the BP. Fig. 9(a) illustrates the utilization of the delayed autoheterodyne method for monitoring the beat frequency, with no occurrence of multimode phenomena observed during the monitoring process. In addition, The outcomes of 500 frequency scans demonstrate that they have consistently remained in a SLM state. This indicates that adding the SA can solve the problem of transient multimode phenomenon. Moreover, wavelength stability is also an important index for evaluating the performance of the laser. The wavelength measurement results of the BEFL using a wavemeter are shown in Fig. 9(b). In 17 hours, the wavelength fluctuation of the BEFL is less than 1.6 pm. It is proved that the BEFL with the SA have a good wavelength stability.

As shown in Fig. 10, the 20-dB bandwidth of the BEFL is measured to be 9.75 kHz. Therefore, 490 Hz can be considered conservative characterization of the laser linewidth. The BEFL with the SA has a good linewidth performance and achieves a sub-kilohertz output.

C. BEFL With the SA and the Self-Injection Feedback Structure

By adding the self-injection feedback structure to BEFL and the structure is shown in Fig. 1. The self-injecting feedback

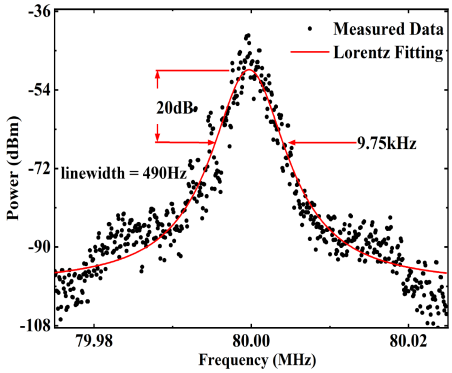

Fig. 10. BEFL with the SA linewidth measurement diagram.

structure has filtering function that makes the intracavity mode purer. Meanwhile, the self-feedback structure also serves as a composite cavity. However, in order to ensure the stable output of the BEFL, it is crucial to match the wavelength of the stokes light with the peak position of the gain spectrum. Regrettably, the self-injection feedback structure and the length of the main cavity are influenced by environmental factors. Consequently, aligning the maximum position of the net gain inside the cavity is difficult. In the experiment, we adjust the wavelength of the BP instead of modify the length of the self-injecting feedback structure. However, due to the influence of environment and temperature on the self-injecting feedback structure, EDFLs exhibits mode hopping phenomenon. The wavelength measurement results of the EDFLs are shown in Fig. 11(a), it can be seen that there are many mode hopping states and the maximum wavelength jump is approximately 0.1 nm. As shown in Fig. 11(b), the wavelength and power of the BP is 1549.304 nm and 7.5 dBm. Consequently, the generation of the SBS occurred in the EDF, yielding a stokes light wavelength of 1549.396 nm and a Brillouin frequency shift of 0.92 nm. At this point, the OSNR of the BEFL is 71 dB. In addition, under a 980 nm pump with the power of 120 mW, the output of the BEFL varies with BP as shown in Fig. 12(a). When the power of the BP is below 3.14 dBm, BP cannot excite the SBS and the output of the laser is EDFLs. Within the power range of 3.14 dBm to 8.32 dBm, SBS was generated in EDF, causing resonation and amplification of the stokes light within the cavity. However, as the power of the BP increases, BP gradually seizes the gain of the EDF, resulting in a reduction in the net gain of the stokes light. Once the power of the BP exceeds 8.32 dBm, BP captures most of the gain, resulting in a significant decrease in the power of the stokes light. As shown in Fig. 12(b), the linewidth of the laser measured by the delayed autoheterodyne method is 224 Hz. This indicates that self-injection feedback structure can reduce the noise of the laser, resulting in better linewidth performance of the laser.

It is worth noting that the wavelength of the BP no longer corresponds to 1549.290 nm. Therefore, the output wavelength of the BEFL has changed. This is primarily attributed to self-injection feedback structure. As a result, the original wavelength of the stokes light may not align with the resonance wavelength of both the main cavity and the self-injection feedback

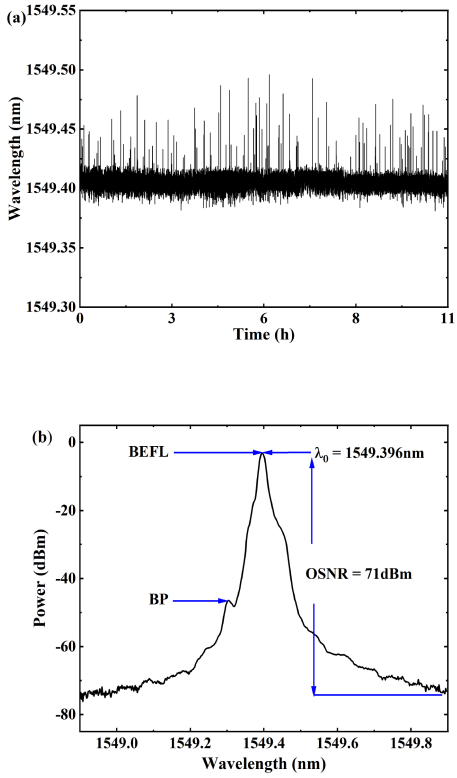

Fig. 11. (a) Wavelength measurement diagram with the SA and the self-injection feedback structure without BP. (b) Spectrogram of BEFL under BP injection.

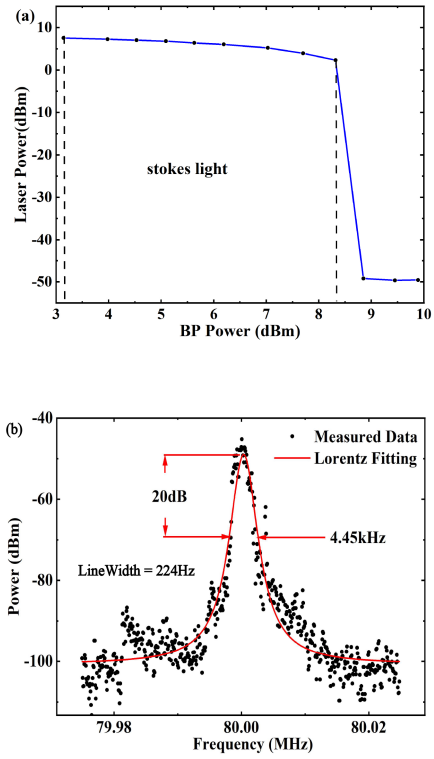

Fig. 12. (a) Power diagram of the BEFL. (b) Line width fitting diagram of the BEFL.

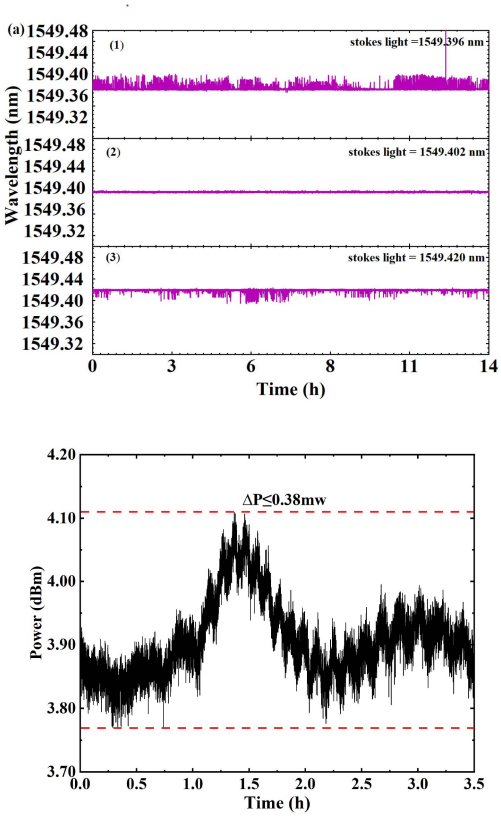

Fig. 13. (a) Wavelength diagram of the BEFL under the different BP wavelengths (b) Output power diagram of the BEFL under 7.5 dBm BP and 120 mw pump.

structure, leading to unstable output of the laser. In order to reduce experimental complexity, adjusting the wavelength of the BP instead of adjusting the length of the self-injection feedback structure. As shown in Fig. 13(a), the state diagrams of the stokes light wavelength were tested under different BP powers. The figure shows that when adjusting the wavelength of the stokes light to 1549.396 nm and 1549.420 nm, several occurrences of mode hopping were observed over a 14 hours monitoring period. When the wavelength of the stokes light is 1549.402 nm, the output wavelength of the laser is relatively stable. The wavelength fluctuation is less than 4.5 pm within 14 hours of detection. This indicates that the wavelength of the BP plays a crucial role in the stability of the laser output. Furthermore, the self-injecting feedback structure has a filtering function, but the added complexity of the system degrades the wavelength stability. This is mainly because the length of the self-injection feedback structure composed of fibers changes with temperature and vibration, which leads to jitter in the net gain of stokes light and cannot effectively suppress other modes in the cavity. Therefore, using physically stable structures can further improve wavelength stability performance. However, it is worth sacrificing wavelength stability appropriately to obtain narrower linewidth for BEFL. The results of the output power of the BEFL are shown in Fig. 13(b). Within 3.5 hours, the power fluctuation of the laser is less than 0.435 mW, indicating that the entire laser has good power performance. The main parameters

TABLE I
PERFORMANCE TABLE FOR THREE TYPES OF LASER STRUCTURES

Type	SLM	Wavelength stability	line-width
Basic structure	instability	-	900 Hz
Single SA	Stable	$\leq$ 1.6 pm	490 Hz
SA and feedback	Stable	$\leq$ 4.5 pm	224 Hz

of the three structures are shown in Table I. SA ensures the SLM operation of the laser and has the effect of narrowing the linewidth. The feedback structure has a filtering effect, making the intracavity mode more pure.

IV. CONCLUSION

In conclusion, an all-PM BEFL with the SA and the self-injection feedback structure has been proposed and demonstrated. The effectiveness of the SA and the self-injection feedback structure are compared and analyzed based on the free-running BEFL. The experimental result proves that the SA structure can eliminate multimode phenomena and narrow the linewidth, while the self-injecting feedback structure can filter out the mode in the cavity effectively. Finally, the maximum fluctuation of the all-PM BEFL wavelength is 4.5 pm within 14 hours, and the linewidth of the BEFL is 224 Hz. It is worth noticing that the whole BEFL is exposed to the air environment without encapsulation, temperature control and other vibration isolation. Therefore, the stability and robustness of the BEFL can be further improved after the BEFL being packaged and vibration isolated.

REFERENCES

[1] D. Psaltis, "Coherent optical information systems," *Science*, vol. 298, pp. 1359–1363, 2002.
[2] X. Zhang, W. Diao, Y. Liu, J. Liu, X. Hou, and W. Chen, "Single-frequency polarized eye-safe all-fiber laser with peak power over kilowatt," *Appl. Phys.*, vol. 115, pp. 123–127, 2014.
[3] C. Liu et al., "GVD-insensitive stable radio frequency phase dissemination for arbitrary-access loop link," *Opt. Exp.*, vol. 24, no. 20, pp. 23376–23382, 2016.
[4] Y. L. Yu, S. K. Liaw, W. C. Hsu, M. H. Shih, and N. K. Chen, "Single longitudinal mode ytterbium doped fiber lasers with large proposed tuning range," *Opt. Quantum. Electron.*, vol. 47, pp. 131–137, 2015.
[5] S. Mo et al., "600-Hz linewidth short-linear-cavity fiber laser," *Opt. Lett.*, vol. 39, no. 20, pp. 5818–5821, 2014.
[6] C.-H. Yeh, Z.-Q. Yang, T.-J. Huang, C.-W. Chow, Y.-J. Chang, and M.-J. Chen, "Erbium-doped fiber dual-ring laser with stable single-longitudinal-mode and 55-nm tuning range," *Opt Laser. Technol.*, vol. 106, pp. 119–122, 2018.
[7] N. Pourshab, A. Gholami, M. J. Hekmat, and N. Shahriyari, "Analysis of narrow linewidth fiber laser using double subring resonators," *J. Opt. Soc. Amer. B*, vol. 34, no. 11, pp. 2414–2420, 2017.
[8] C. Spiegelberg, J. Geng, Y. Hu, Y. Kaneda, S. Jiang, and N. Peyghambarian, "Low-noise narrow-linewidth fiber laser at 1550 nm," *J. Light. Technol.*, vol. 22, no. 1, pp. 57–62, Jan. 2004.
[9] Y. O. Barmenkov, D. Zalvidea, S. Torres-Peiró, J. L. Cruz, and M. V. Andrés, "Effective length of short Fabry-Perot cavity formed by uniform fiber Bragg gratings," *Opt. Exp.*, vol. 14, no. 14, pp. 6394–6399, 2006.
[10] X. Cen et al., "Short-wavelength, in-band-pumped single- frequency DBR tm^{3+}-doped germanate fiber laser at 1.7 μm," *IEEE Photon. Technol. Lett.*, vol. 33, no. 7, pp. 350–353, Apr. 2021.
[11] H.-C. Chien, C.-H. Yeh, C.-C. Lee, and S. Chi, "A tunable and single-frequency S-band erbium fiber laser with saturable-absorber-based auto-tracking filter," *Opt. Commun.*, vol. 250, no. 1-3, pp. 163–167, 2005.
[12] X. Zhang, N. H. Zhu, L. Xie, and B. X. Feng, "A stabilized and tunable single-frequency erbium-doped fiber ring laser employing external injection locking," *J. Light. Technol.*, vol. 25, no. 4, pp. 1027–1033, Apr. 2007.

[13] X. He, D. N. Wang, and C. R. Liao, "Tunable and switchable dual-wavelength single-longitudinal-mode erbium-doped fiber lasers," *J. Light. Technol.*, vol. 29, no. 6, pp. 842–849, Mar. 2011.

[14] Z. Wang, J. Shang, K. Mu, Y. Qiao, and S. Yu, "Single-longitudinal-mode fiber laser with an ultra-narrow linewidth and extremely high stability obtained by utilizing a triple-ring passive subring resonator," *Opt Laser. Technol.*, vol. 130, 2020, Art. no. 106329.

[15] X. Chen, J. Yao, F. Zeng, and Z. Deng, "Single-longitudinal-mode fiber ring laser employing an equivalent phase-shifted fiber Bragg grating," *IEEE Photon. Technol. Lett.*, vol. 17, no. 7, pp. 1390–1392, Jul. 2005.

[16] V. Spirin et al., "Sub-kilohertz Brillouin fiber laser with stabilized self-injection locked DFB pump laser," *Opt. Laser. Technol.*, vol. 141, 2021, Art. no. 107156.

[17] Y. Pang, Y. Xu, X. Zhao, Z. Qin, and Z. Liu, "Low-noise Brillouin random fiber laser with auto-tracking dynamic fiber grating based on a saturable absorption ring," *Infrared. Phys. Technol.*, vol. 122, 2022, Art. no. 104088.

[18] Y. Pang, Y. Xu, X. Zhao, Z. Qin, and Z. Liu, "Stabilized narrow-linewidth Brillouin random fiber laser with a double-coupler fiber ring resonator," *J. Light. Technol.*, vol. 40, no. 9, pp. 2988–2995, May 2022.

[19] S. Huang et al., "Tens of hertz narrow-linewidth laser based on stimulated Brillouin and Rayleigh scattering," *Opt. Lett.*, vol. 42, no. 24, pp. 5286–5289, 2017.

[20] M. Chen, Z. Meng, and H. Zhou, "Low-threshold, single-mode, compact Brillouin/erbium fiber ring laser," *J. Light. Technol.*, vol. 31, no. 12, pp. 1980–1986, Jun. 2013.

[21] Z. Wang, J. Shang, J. Yang, Y. Xu, Y. Qiao, and S. Yu, "All polarization maintaining single-longitudinal-mode Brillouin/erbium fiber laser with ultra-narrow linewidth and high stability," *Opt. Fiber. Technol.*, vol. 71, 2022, Art. no. 102928.

[22] K. Zhang and J. U. Kang, "C-bandwavelength-swept single-longitudinal mode erbium-doped fiber ring laser," *Opt. Exp.*, vol. 16, pp. 14173–14179, 2008.

[23] A. Othonos, K. Kalli, and G. E. Kohnke, "Fiber Bragg gratings: Fundamentals and applications in telecommunications and sensing," *Mater. Today Phys.*, vol. 53, pp. 61–62, 2000.

[24] T. M. Wang, L. Zhang, C. Feng, M. Qin, and L. Zhan, "Tunable bistability in hybrid Brillouin–erbium single-frequency fiber laser with saturable absorber," *Mater. Today Phys.*, vol. 33, no. 8, pp. 1635–1639, 2016.

[25] T. Feng et al., "Four-wavelength-switchable SLM fiber laser with sub-kHz linewidth using superimposed high-birefringence FBG and dual-coupler ring based compound-cavity filter," *Opt. Exp.*, vol. 27, no. 25, pp. 36662–36679, 2019.

[26] L. F. Stokes, M. Chodorow, and H. J. Shaw, "All-single-mode fiber resonator," *Opt. Lett.*, vol. 7, no. 6, pp. 288–290, 1982.

[27] Z. Wang, J. Shang, S. Li, K. Mu, Y. Qiao, and S. Yu, "All-polarization maintaining single-longitudinal-mode fiber laser with ultra-high OSNR, sub-kHz linewidth and extremely high stability," *Opt. Laser Technol.*, vol. 141, 2021, Art. no. 107135.

[28] S. Huang, T. Zhu, and G. Yin, "Dual-cavity feedback assisted DFB narrow linewidth laser," *Sci. Rep.*, vol. 7, 2017, Art. no. 1185.

[29] Y. Liu, J.-L. Yu, W.-R. Wang, H.-G. Pan, and E.-Z. Yang, "Single longitudinal mode Brillouin fiber laser with cascaded ring Fabry–Pérot resonator," *IEEE Photon. Technol. Lett.*, vol. 26, no. 2, pp. 169–172, Jan. 2014.

[30] H. Ludvigsen, M. Tossavainen, and M. Kaivola, "Laser linewidth measurements using self-homodyne detection with short delay," *Opt. Commun.*, vol. 155, pp. 180–186, 1998.